RESEARCH ARTICLE

Fundamental losses in solar cells

Louise C. Hirst* and Nicholas J. Ekins-Daukes

Department of Physics, Imperial College London, London SW7 2AZ, UK

ABSTRACT

This paper considers intrinsic loss processes that lead to fundamental limits in solar cell efficiency. Five intrinsic loss processes are quantified, accounting for all incident solar radiation. An analytical approach is taken to highlight physical mechanisms, obscured in previous numerical studies. It is found that the free energy available per carrier is limited by a Carnot factor resulting from the conversion of thermal energy into entropy free work, a Boltzmann factor arising from the mismatch between absorption and emission angles and also carrier thermalisation. It is shown that in a degenerate band absorber, a free energy advantage is achieved over a discrete energy level absorber due to entropy transfer during carrier cooling. The non-absorption of photons with energy below the bandgap and photon emission from the device are shown to be current limiting processes. All losses are evaluated using the same approach providing a complete mathematical and graphical description of intrinsic mechanisms leading to limiting efficiency. Intrinsic losses in concentrator cells and spectrum splitting devices are considered and it is shown that dominant intrinsic losses are theoretically avoidable with novel device designs. Copyright © 2010 John Wiley & Sons, Ltd.

*Correspondence

Louise C. Hirst, Department of Physics, Imperial College London, London SW7 2AZ, UK.

E-mail: louise.hirst@imperial.ac.uk

1. INTRODUCTION

Fundamental limiting efficiency has been discussed by many authors with several analyses being presented. Shockley and Queisser published a detailed balance approach, using the generalised Planck formalism to identify current–voltage characteristics, with the maximum power point giving the fundamental limiting efficiency [1,2]. Other authors have derived consistent results from a thermodynamic approach. By considering energy and entropy fluxes, limits to photovoltaic conversion are established [3,4]. This paper considers intrinsic loss processes which lead to fundamental limiting efficiency and how these change in different device designs.

Loss processes occurring in a single bandgap device under one sun illumination can be divided into two distinct categories. Extrinsic losses, such as series resistance, parasitic recombination and contact shadowing, can substantially limit device efficiency; however, they are theoretically avoidable and consequently are not considered when calculating fundamental limiting efficiency. Intrinsic losses are unavoidable in this device design and will still be present in an idealised solar cell [5]. This paper assumes five intrinsic loss processes. The mismatch between the broad solar spectrum and the mono-energetic absorption of a single bandgap (E_g) results in the non-absorption of photons with energy below the bandgap (i, below E_g loss). This mismatch along with a strong interaction between excited carriers and lattice phonons introduces a thermalisation loss as carriers cool to the bandgap edge (ii, thermalisation loss). According to Kirchoff's law, absorbers must also be emitters and as such cell emission further reduces conversion efficiency (iii, emission loss). A solar cell can be considered as a heat engine with heat flowing from a hot reservoir (the Sun) to a cold reservoir (the atmosphere) doing work in the process. The conversion of thermal energy into electrical work requires some energy to be sacrificed to the cold reservoir and hence will always incur an energy penalty [6]. In a solar cell, this loss manifests itself as a voltage drop referred to as the Carnot factor (iv, Carnot loss). Landsberg and Markvart have quantified this loss for a two level system [7]. Finally, the inequality of absorption and emission angles results in an entropy generation process because of the expansion of photon modes (v, Boltzmann loss). Mis-

matched optical étendue introduces irreversibility which limits conversion efficiency [2,8].

This paper uses an analytical approach to quantify the five intrinsic losses. These losses are shown to define the form of a device's current–voltage characteristic. The effects of concentration and E_g on intrinsic loss processes are discussed and a novel graphical representation of losses in a solar cell, accounting for all incident solar radiation, is presented allowing the mechanisms leading to limiting efficiency to be visualised.

2. ANALYTICAL SOLUTION TO THE GENERALISED PLANCK EQUATION

The Sun can be modelled as a blackbody, radially emitting a spectrum uniquely described by its temperature ($T = 6000\,\mathrm{K}$). A small solid angle of the Sun's thermal radiation reaches the earth and can be used to produce electricity in photovoltaic solar cells. A solar cell will emit a luminescent spectrum described by the temperature of the device and the voltage across it. The generalised Planck equation incorporates the effect of chemical potential (μ) on emission to calculate the total photon emission flux ($n(E, T, \mu, \Omega)$) per energy interval (dE) per unit solid angle (Ω) (Equation (1)). It can be derived from either a statistical [9] or thermodynamic basis [5].

$$n(E, T, \mu, \Omega) = \frac{2\Omega}{c^2 h^3} \frac{E^2}{e^{\left(\frac{E-\mu}{kT}\right)} - 1} \qquad (1)$$

T is the temperature of the emitting body, c is the speed of light, h is Planck's constant and k is Boltzmann's constant. In the case of thermal emission, such as solar radiation, $\mu = 0$; however, luminescent emission from a photovoltaic device has $\mu = eV$, where e is the electron charge and V is the voltage across the device.

A detailed balance approach uses the generalised Planck to calculate the photocurrent as the difference between absorbed and emitted photons (Equation (2)).

$$J = e \int_{E_g}^{\infty} n(E, T_S, 0, \Omega_{\mathrm{abs}}) dE - e \int_{E_g}^{\infty} n(E, T_A, \mu, \Omega_{\mathrm{emit}}) dE \qquad (2)$$

Ω_{abs} and Ω_{emit} refer to the solid angles of absorption and emission, respectively. T_S and T_A refer to the temperature of the Sun and the absorber, respectively. This article assumes an abrupt absorption threshold and so integration is over the energy range $E_g \to \infty$ as photons with energy below E_g are transmitted. The product of J and V gives the electrical power output. Device efficiency is, therefore, calculated as shown in Equation (3), where P_{in} describes the incident solar energy current.

$$\eta = \frac{JV}{P_{\mathrm{in}}} \qquad (3)$$

Efficiency is described by two independent variables: E_g and V; therefore finding the maximum achievable efficiency is calculated by evaluating two partial differential equations (Equations (4) and (5)).

$$\left(\frac{\partial \eta}{\partial E_g}\right)_V = 0 \qquad (4)$$

$$\left(\frac{\partial \eta}{\partial V}\right)_{E_g} = 0 \qquad (5)$$

2.1. Deriving the optimal operating voltage

An analytical solution to Equation (4) is found by taking the Boltzmann approximation, neglecting the -1 in the denominator of the generalised Planck equation. This solution provides a relationship between the optimal operating voltage (V_{opt}) and E_g (Equation (6)).

$$eV_{\mathrm{opt}} = E_g \left(1 - \frac{T_A}{T_S}\right) - T_A k \ln\left(\frac{\Omega_{\mathrm{emit}}}{\Omega_{\mathrm{abs}}}\right) \qquad (6)$$

The first term in Equation (6) is the Carnot factor previously derived in this manner by Landsberg and Badescu [10]. The second term is here referred to as the Boltzmann factor because it takes the form of Boltzmann's equation representing entropy generation with increased occupancy of available states, $\Delta S = k \ln(\Omega_{\mathrm{emit}}/\Omega_{\mathrm{abs}})$. The energy flow associated with that entropy generation is given by $T\Delta S$. Markvart's study of the thermodynamics of optical étendue derives this term from a different basis [11]. The relation shown in Equation (6) shows that the useful work available per carrier is limited by unavoidable heat loss to the surroundings (Carnot factor) and irreversible entropy generation (Boltzmann factor).

2.2. Justifying approximations

2.2.1. Optimal voltage approximation.

Under maximum concentration ($\Omega_{\mathrm{abs}} = \Omega_{\mathrm{emit}}$), the Boltzmann factor tends to zero. Under this condition, the value of V_{opt} will be exact for a device with optimal bandgap, when the condition in Equation (5) is also satisfied. Away from this value, V_{opt} is only approximate. The accuracy of this approximation is shown in Figure 1, where the approximate analytical solution for V_{opt}/E_g is plotted alongside an exact numerical calculation for a cell under maximum concentration. The two equate at the optimal bandgap for this concentration. Analytically calculated V_{opt} is lower than the numerical calculation for devices with E_g below the optimal, and higher for devices with E_g above the optimal. Within 0.1 eV of the optimal bandgap, analytical and numerical solutions differ by <0.004Eg eV.
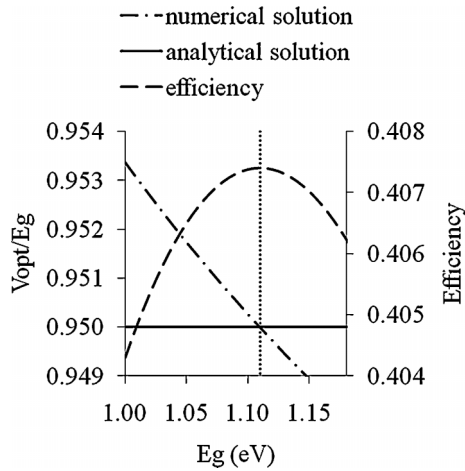
Figure 1. An approximate analytical solution for V_{opt}/E_g is compared to an exact numerical calculation for a cell under maximum concentration. The two equate at the optimal bandgap for this concentration.

2.2.2. Boltzmann approximation.

At low energies, the effect of the -1 in the denominator of the generalised Planck (Equation (1)) becomes significant and the Boltzmann approximation is no longer valid. In the regime of realistic bandgaps ($E_g > 0.5\,\text{eV}$), taking the Boltzmann approximation has a negligible effect on the calculation of V_{opt} (Figure 2a). The Boltzmann approximation has a more significant effect on current calculation (Figure 2b). Total incident photon flux calculated with the approximation is 83% of that calculated without. Absorbed photon flux is calculated in the same way and so will be lower than its true value for low E_g devices; however, with increasing E_g, analytical values for absorbed photon flux tend to their numerical values. Device efficiency is a function of the ratio of absorbed photon flux to total incident photon flux and as such inaccuracies in current calculation, deriving from the Boltzmann approximation, cancel out for low E_g devices. With increasing E_g, cancellation does not take place and so device efficiencies appear slightly higher than their numerical counterparts.
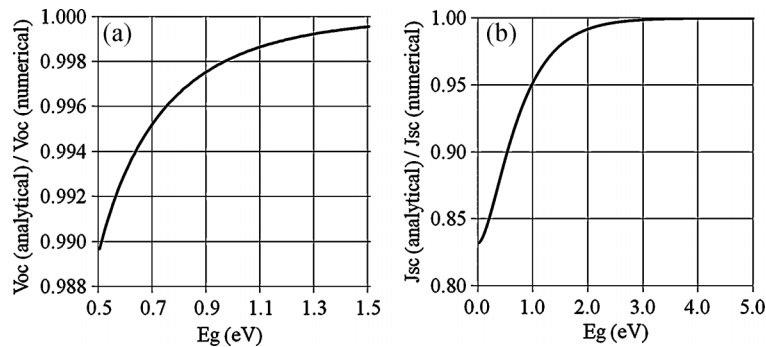
The net effect of these approximations is for analytically calculated efficiencies to appear slightly lower than their numerically calculated values for low E_g devices and slightly higher for high E_g devices.

2.3. Deriving open circuit voltage

Under the conditions of open circuit voltage (V_{oc}), no current flows. V_{oc} can, therefore, be derived by equating Equation (2) to zero. Taking the Boltzmann approximation and integrating by parts gives Equation (7).

$$\exp\left\{\frac{eV_{oc}}{kT_A}\right\} = \frac{\Omega_{abs}}{\Omega_{emit}}\frac{\gamma(E_g, T_S)}{\gamma(E_g, T_A)}\exp\left\{\frac{E_g}{kT_A}\left(1 - \frac{T_A}{T_S}\right)\right\} \tag{7}$$

which yields

$$eV_{oc} = E_g\left(1 - \frac{T_A}{T_S}\right) - kT_A\ln\left(\frac{\Omega_{emit}}{\Omega_{abs}}\right)$$
$$+ kT_A\ln\left(\frac{\gamma(E_g, T_S)}{\gamma(E_g, T_A)}\right) \tag{8}$$

$$\gamma(E, T) = \frac{2kT}{c^2h^3}\left(E^2 + 2kTE + 2k^2T^2\right) \tag{9}$$

The first and second terms of Equation (8) are the Carnot and Boltzmann factors, respectively. The third term describes an increase in the free energy per carrier. This occurs as a result of the mismatch between the temperatures of the absorbed and emitted photon distributions [11]. The strong interaction between excited carriers and lattice phonons results in heat transferring from the carrier distribution to the lattice. Entropy is also transferred to the lattice in this cooling process, decreasing the entropy of the excited carrier population. The total entropy of the electron population and the lattice combined still increases, in accordance with the second law of thermodynamics. The free energy available in the carrier distribution can be described by Helmholtz free energy (Equation (10)), where H is the Helmholtz free energy of the carrier distribution, U is the internal energy of the carrier distribution, T is the temperature of the carrier

Figure 2. (a) The ratio of V_{oc} (calculated analytically) to V_{oc} (calculated numerically) is shown as a function of E_g. (b) the ratio of J_{sc} (calculated analytically) to J_{sc} (calculated numerically) is shown as a function of E_g.

distribution and S is the entropy of the carrier distribution.

$$H = U - TS \qquad (10)$$

The cooling of carriers reduces U; however, some of this loss is recouped because the corresponding reduction in T and S results in the slight increase in free energy available per carrier described in the third term of Equation (8). The degenerate nature of absorption bands enables this free energy advantage and as such, the free energy available per carrier in a discrete energy level absorber is lower.

3. COMPARING DEGENERATE AND DISCRETE ABSORBERS

In a two level discrete absorber, carrier cooling does not occur because in an infinitely narrow absorption band all carriers are absorbed and emitted with the same energy (monochromatic light). The increase in available free energy per carrier as a result of cooling, described in the third term of Equation (8), is zero for a discrete absorber. Equation (11) describes current flow in a device with two energy levels of finite width ΔE, separated by E_{12} (Figure 3). In the limit $\Delta E \rightarrow 0$, Equation (11) can be evaluated analytically as shown in Equation (12).

$$J_{E_{12}} = e \int_{E_{12}}^{E_{12}+2\Delta E} n(E, T_S, 0, \Omega_{abs})dE$$

$$- e \int_{E_{12}}^{E_{12}+2\Delta E} n(E, T_A, \mu, \Omega_{emit})dE \qquad (11)$$

$$J_{E_{12}} = \frac{2E_{12}^2 e}{c^2 h^3} \left(\Omega_{abs} \exp\left(\frac{-E_{12}}{kT_S}\right) \right.$$

$$\left. - \Omega_{emit} \exp\left(\frac{eV - E_{12}}{kT_A}\right) \right) \Delta E \qquad (12)$$

Taking $J_{E_{12}} = 0$ yields,

$$eV_{oc} = E_{12}\left(1 - \frac{T_A}{T_S}\right) - kT_A \ln\left(\frac{\Omega_{emit}}{\Omega_{abs}}\right) \qquad (13)$$
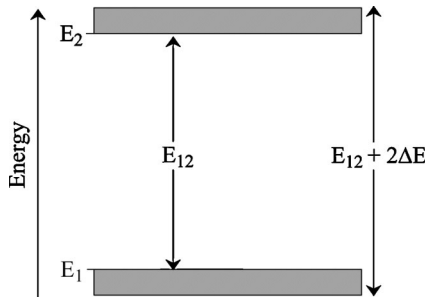
Figure 3. An absorber with two energy levels of thickness ΔE, separated by E_{12}. As $\Delta E \rightarrow 0$ the system becomes a discrete absorber.
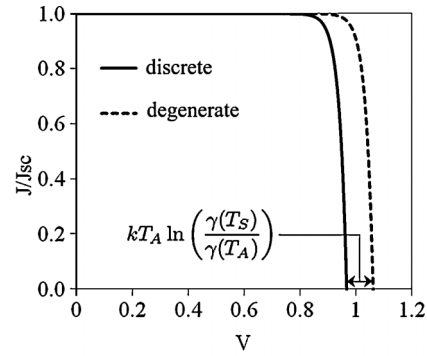
Figure 4. Normalised J–V curves for discrete and degenerate absorbers with $E_{12} = E_g = 1.31$ eV under one sun illumination. V_{oc} is higher for the degenerate absorber because of the entropy transfer occurring as a result of carrier cooling.

Comparing Equations (8) and (13) shows that the free energy per carrier is greater in a degenerate system because carrier cooling results in entropy transfer away from the carrier distribution (Figure 4).

4. CURRENT–VOLTAGE CHARACTERISTICS

All loss processes result in either a reduction in current or a reduction in voltage. Below E_g loss and emission loss limit the number of available carriers and as such are current drop processes. Thermalisation, Boltzmann and Carnot losses all reduce the energy with which carriers can be extracted and, therefore, are voltage drop processes. Reductions in current and voltage due to intrinsic losses are shown in Figure 5 for a device under one sun illumination. The total area gives
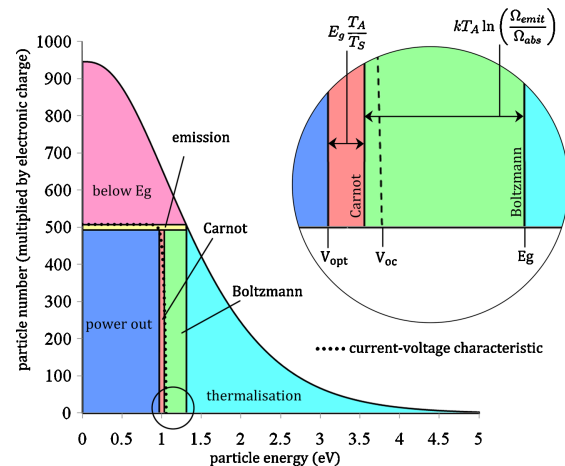
Figure 5. Intrinsic losses occurring in a device with optimal E_g (1.31 eV) under one sun illumination. Carnot, Boltzmann and thermalisation losses reduce optimal operating voltage where as below E_g and emission losses reduce current, dictating the form of the current–voltage characteristic. Analytical descriptions of Carnot and Boltzmann voltage drops are given.

Table I. All mechanisms are analytically described. $\chi(E, T)$ and J_{opt} are represented in Equations (20) and (21), respectively.

Below E_g	$\int_0^{E_g} E \cdot n(E, T_S, 0, \Omega_{abs}) \, dE \approx \Omega_{abs} \left(\chi(0, T_S) - \exp\left(-\dfrac{E_g}{kT_S}\right) \chi(E_g, T_S) \right)$	(14)
Thermalisation loss	$\int_{E_g}^{\infty} E \cdot n(E, T_S, 0, \Omega_{abs}) \, dE - E_g \int_{E_g}^{\infty} n(E, T_S, 0, \Omega_{abs}) \, dE \approx \Omega_{abs} \exp\left(-\dfrac{E_g}{kT_S}\right) \left(\chi(E_g, T_S) - E_g \cdot \gamma(E_g, T_S) \right)$	(15)
Emission loss	$E_g \int_{E_g}^{\infty} n(E, T_A, eV_{opt}, \Omega_{emit}) \, dE \approx \Omega_{emit} E_g \gamma(E_g, T_A) \exp\left(\dfrac{eV_{opt} - E_g}{kT_A}\right)$	(16)
	substitute Equation (6) $\approx \Omega_{abs} E_g \gamma(E_g, T_A) \exp\left(\dfrac{-E_g}{kT_S}\right)$	
Boltzmann loss	$kT_A \ln\left(\dfrac{\Omega_{emit}}{\Omega_{abs}}\right) J_{opt}$	(17)
Carnot loss	$E_g \left(\dfrac{T_A}{T_S}\right) J_{opt}$	(18)
Power out	$J_{opt} V_{opt}$	(19)

the power in the incident solar spectrum. The areas of the different shaded regions give the power attributed to the different intrinsic loss processes. Once all current and voltage drop processes are accounted for, the current–voltage characteristic of the device is derived.

5. ACCOUNTING FOR ALL THE SUN'S ENERGY

An analytical approach has been used to quantify all intrinsic losses and to calculate power out (Table I).

$$\chi(E, T) = \frac{2kT}{c^2 h^3} (E^3 + 3E^2 kT + 6E k^2 T^2 + 6k^3 T^3) \quad (20)$$

$$J_{opt} = e \int_{E_g}^{\infty} n(E, T_S, 0, \Omega_{abs}) \, dE$$

$$- e \int_{E_g}^{\infty} n(E, T_A, eV_{opt}, \Omega_{emit}) \, dE$$

$$\approx e\Omega_{abs} \gamma(E_g, T_S) \exp\left(\frac{-E_g}{kT_S}\right)$$

$$- e\Omega_{emit} \gamma(E_g, T_A) \exp\left(\frac{eV_{opt} - E_g}{kT_A}\right)$$

substitute Equation (6)

$$\approx e\Omega_{abs} \left[\gamma(E_g, T_S) \exp\left(\frac{-E_g}{kT_S}\right) \right.$$

$$\left. - \gamma(E_g, T_A) \exp\left(\frac{-E_g}{kT_S}\right) \right] \quad (21)$$

In order to calculate the fraction of incident solar radiation a loss process consumes or to calculate device efficiency, equations in Table I should be divided by total incident solar energy current P_{in} (Equation (22)).

$$P_{in} = \int_0^{\infty} E \cdot n(E, T_S, 0, \Omega_{abs}) \, dE$$

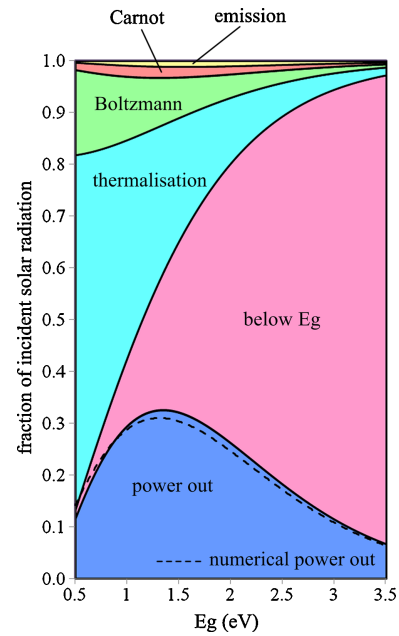$$\approx \Omega_{abs} \chi(0, T_S) \quad (22)$$

Figure 6. Intrinsic loss processes and hence, power out are shown to be dependent on E_g. All incident radiation is accounted for, illustrating why intrinsic loss mechanisms lead to fundamental limiting efficiency.

All incident solar radiation is accounted for, so that the mechanisms leading to limiting efficiency are fully described. Losses and power out are plotted with varying E_g in Figure 6. It should be noted that these results are approximate. Away from the optimal bandgap, the value of V_{opt} used is not exact as shown in Figure 1. In addition, the Boltzmann approximation has been taken to enable an analytical solution. Device efficiencies calculated with and without Boltzmann approximations in the region $0.5 \, \text{eV} < E_g < 3.5 \, \text{eV}$ differ by a maximum of 1.9%. In Figure 6, a numerical solution for power out is shown alongside the analytical solution to show that the combined effect of these approximations is small.

The device efficiency shown in Table II is comparable to the device efficiency calculated analytically by Shock-

Table II. The fraction of incident solar energy attributed to different mechanisms for a device under one sun illumination with $E_g = 1.31$ eV. It should be noted that maximum power out occurs at $E_g = 1.35$ eV in this analytical model; however, values at 1.31 eV are shown to allow comparison with numerical models.

Mechanism	Efficiency at $E_g = 1.31$ eV
Power out	0.325
Below E_g loss	0.250
Thermalisation loss	0.298
Carnot loss	0.022
Boltzmann loss	0.093
Emission loss	0.011

ley and Queisser [1], 0.31 at $E_g = 1.31$ eV. Thermalisation and below E_g are the dominant loss processes (Table II). Thermalisation loss reduces with increasing bandgap while below E_g loss increases. This is because increasing the bandgap reduces the number of absorbed photons while increasing the energy with which they can be extracted. Boltzmann loss is also a substantial loss mechanism, resulting in a 9.3% efficiency reduction at $E_g = 1.31$ eV.

5.1. Implications for solar cell design

The five intrinsic losses modelled in this paper are unavoidable in the single junction semiconductor device under one sun illumination; however, changing device design enables some of these losses to be avoided. The fundamental limiting efficiency of this cell design is far from the ultimate limiting efficiency of solar energy conversion. A simple design enhancement is to concentrate incident solar radiation onto a solar cell using lenses or mirrors. This reduces the voltage drop associated with the Boltzmann loss, increasing efficiency. The same effect can be achieved in a device with restricted angular emission. Figure 7 shows how the fraction of solar energy which can be extracted as useful work varies with concentration for fixed E_g. Under 215 times concentration, the fraction of incident solar energy lost because of absorption as emission angle mismatch is half that at one sun. The fraction of incident solar radiation lost via other intrinsic loss processes is independent of absorption and emission angles as can be seen by dividing equations in Table I by Equation (22).

Advanced solar cell concepts offer the potential for substantial efficiency improvement by limiting the dominant loss mechanisms [12]. In a hot carrier solar cell, interactions between excited electrons and lattice phonons are impeded and the electron population temperature remains higher than that of the lattice. In an idealised hot carrier solar cell, discrete energy selective contacts extract these hot carriers eliminating thermalisation loss [13]. The objective of reducing thermalisation loss is to increase efficiency; however, it cannot be assumed that any reduction in thermalisation loss directly translates to an efficiency improvement. The structure of a hot carrier solar cell is likely to be quite different
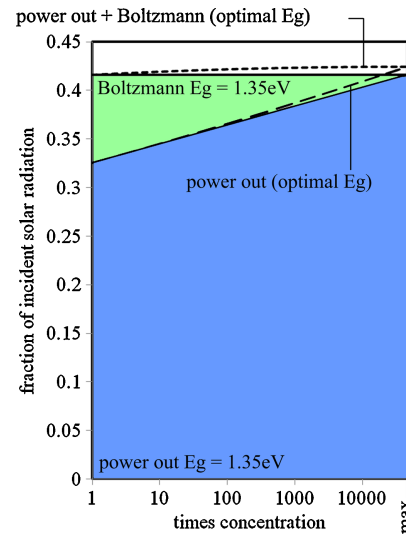

Figure 7. Boltzmann loss and power out are shown for fixed $E_g = 1.35$ eV, which is the optimal E_g in this model for a device under one sun illumination. Increasing concentration reduces the mismatch between absorption and emission angles and the resulting reduction in Boltzmann loss is directly transferred into power out. Increasing concentration alters optimal E_g and so Boltzmann loss and power out are also shown for optimal E_g at each concentration. When E_g is not fixed, Boltzmann loss and power out no longer sum to a constant value over the full range of concentration. This is an artefact of the analytical model used occurring because changes in E_g affect the accuracy of the Boltzmann approximation.

from the model outlined in this paper and so other intrinsic loss mechanisms might also be affected.

Substantial efficiency advantages can be achieved by splitting the broad solar spectrum into spectral elements [5,14]. In a multijunction device, each element is converted in a material with a different bandgap. This can be implemented in spectrum splitting or stacked cell designs. Figure 8 shows loss mechanisms in a double junction, unconstrained device under one sun illumination. The different shaded areas give the power attributed to different mechanisms and sum to the total power in the solar spectrum. Losses are shown to result in either a reduction in current or voltage determining the form of the current–voltage characteristics. Equations in Table I were used to quantify losses in multijunction devices. Figure 9 shows how the fraction of solar radiation lost via different mechanisms changes with varying junction number. Increasing the number of junctions is thermodynamically equivalent to increasing the number of heat engines and as such Carnot, Boltzmann and emission losses increase. In multijunction devices, the high energy region of the spectrum is converted in an absorber with high bandgap, reducing thermalisation losses. Low bandgap materials are used to absorb the low energy region of the spectrum, reducing below E_g loss.

Reducing device temperature and operating voltage will reduce emission loss; however, the energy penalty associ-
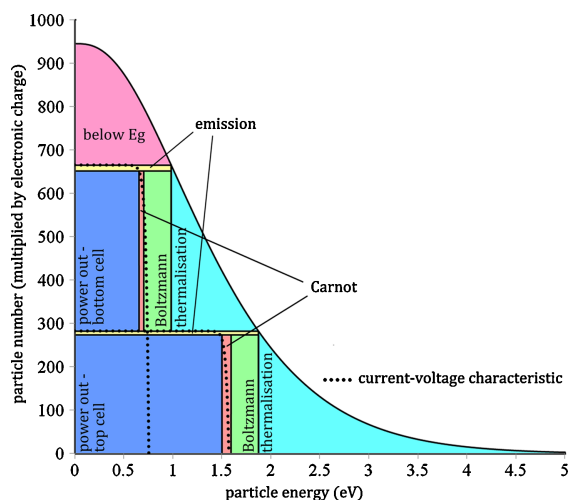
Figure 8. Intrinsic losses occurring in an unconstrained double junction device with optimal bandgaps (0.98 and 1.87 eV) under one sun illumination. Carnot, Boltzmann and thermalisation losses reduce optimal operating voltage in each absorber. The non-absorption of below E_g photons and emission losses reduce current, dictating the form of the current-voltage characteristics.
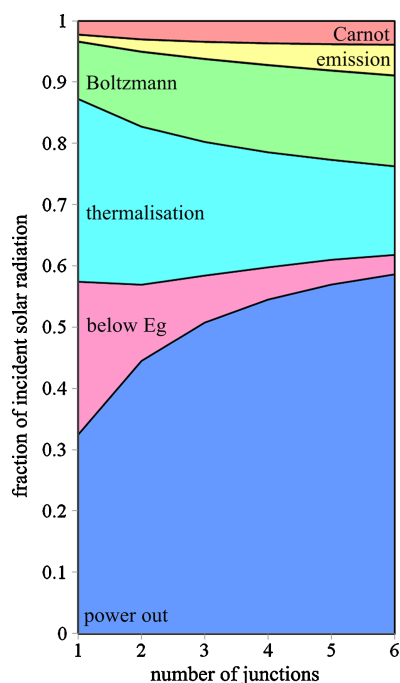

Figure 9. Loss processes and power out in an unconstrained, multijunction device under one sun illumination are shown. All incident solar radiation is accounted for. Optimal bandgaps are used in each case. All mechanisms are shown to be dependent on the number of junctions.

Table III. The efficiency of multijunction devices calculated using an analytical approach are shown alongside values calculated numerically as shown in [15]. Discrepancies of up to 1.7% occur because of approximations made.

number of junctions	power out (analytical)	power out (numerical) [15]
2 (0.98, 1.87 eV)	0.446	0.429
3 (0.82, 1.44, 2.26 eV)	0.508	0.493
4 (0.72, 1,21, 1.77, 2.55 eV)	0.546	0.533

ated with these measures outweighs any potential benefit. One way in which emission loss might be reduced is by overcoming Kirchoff's Law using a time asymmetric absorber. The application of this non-reciprocal system to photovoltaic devices has been considered by several authors [16-18]. Carnot factor will only be eliminated in the limit of an infinite temperature gradient between the Sun and the absorber; however, systems with a cooler heat sink such as extra-terrestrial cells will have reduced Carnot loss.

6. CONCLUSION

Intrinsic losses occurring in a single threshold solar cell under one sun illumination have been considered in this paper. Radiation emitted and absorbed by the cell has been evaluated using the generalised Planck equation. By solving this equation analytically the mechanics of intrinsic loss processes become apparent. Five intrinsic loss processes are identified and quantified. Intrinsic losses are shown to cause either a reduction in current or a reduction in voltage, dictating the form of the current–voltage characteristic.

It was found that the optimal operating voltage of a device is limited by an ultimately unavoidable Carnot factor. In converting thermal energy received from the Sun into entropy free electrical work, an energy penalty will always be incurred. This loss process is only eliminated in the limit of an infinite thermal gradient between the Sun and the solar cell. A further intrinsic voltage drop is present in solar cells under one sun illumination. A mismatch between absorption and emission angles causes an expansion of photon modes and a corresponding entropy generation. This loss mechanism is described by Boltzmann's equation linking available states and entropy generation and is avoided in cells under concentration or with restricted emission angle.

In a single junction device, optimal voltage is also limited by the strong interaction between excited carriers and lattice phonons resulting in thermalisation. Third generation designs, such as multijunction and hot carrier solar cells, impede this loss mechanism. Along with other authors, we have shown that increasing the number of absorbers in a multijunction device decreases thermalisation and below E_g losses but increases the fraction of incident solar radiation lost via Carnot, Boltzmann and emission mechanisms resulting in an overall efficiency increase. Some of the energy lost through thermalisation is recouped because of

the mismatch between absorption and emission temperatures ($T_S \neq T_A$). During carrier cooling some entropy is transferred away from the carrier distribution increasing the free energy available per carrier. This process occurs as a result of degenerate absorption bands and we show that an absorber with discrete energy levels will not experience this free energy advantage. Luminescent emission from the cell reduces the number of available carriers, reducing the operating current; however, the primary mechanism of current reduction is the non-absorption of photons with energy below E_g.

The cumulative effect of all five intrinsic loss mechanisms are shown to lead to fundamental limits in efficiency. All incident solar radiation is accounted for, creating a complete picture for solar energy conversion in an ideal device. The analytical approach taken shows the effect of varying device design on limiting efficiency. Increasing concentration reduces the fraction of incident solar energy lost via Boltzmann entropy generation resulting in an increase in device efficiency. Other losses as a fraction of incident solar energy are independent of optical étendue. All loss mechanisms, however, are shown to be dependent on bandgap.

Understanding the origins of loss in ideal solar cells is necessary to improve device efficiency. Quantifying intrinsic losses identifies areas in which substantial efficiency improvements might be achieved, guiding device design and innovation.

ACKNOWLEDGEMENTS

REFERENCES

1. Shockley W, Queisser HJ. Detailed balance limit of efficiency of p-n junction solar cells. *Journal of Applied Physics* 1961; **32**(3): 510–519. DOI: 10.1063/1.1736034

2. Araújo GL, Martí A. Absolute limiting efficiencies for photovoltaic energy conversion. *Solar Energy Materials and Solar Cells* 1994; **33**(2): 213–240. DOI: 10.1016/0927-0248(94)90209-7

3. DeVos A, Landsberg PT, Brauch P, Parrott JE. Entropy fluxes, endoreversibility, and solar energy conversion. *Journal of Applied Physics* 1993; **74**(6): 3631–3637. DOI: 10.1063/1.354503

4. Würfel P. Thermodynamic limitations to solar energy conversion. *Physica E: Low-dimensional Systems and Nanostructures* 2002; **14**(1–2): 18-26. DOI: 10.1016/S1386-9477(02)00355-7

5. Henry CH. Limiting efficiencies of ideal single and multiple energy gap terrestrial solar cells. *Journal of Applied Physics* 1980; **51**(8): 4494–4500. DOI: 10.1063/1.328272

6. Fermi E. *Thermodynamics*. Dover: New York, 1956; 29–45.

7. Landsberg PT, Markvart T. The Carnot factor in solar-cell theory. *Solid-State Electronics* 1998; **42**(4): 657–659. DOI: 10.1016/S0038-1101(97)00253-0

8. Markvart T. Thermodynamics of losses in photovoltaic conversion. *Applied Physics Letters* 2007; **91**(6): 64102–64105. DOI: 10.1063/1.2766857

9. Ruppel W, Würfel P. Upper limit for the conversion of solar energy. *IEEE Transactions on Electron Devices* 1980; **27**(4): 745–750.

10. Landsberg PT, Badescu V. Carnot factor in solar cell efficiencies. *Journal of Applied Physics* 2000; **33**(22): 3004–3008.

11. Markvart T. The thermodynamics of optical étendue. *Journal of Optics A: Pure and Applied Optics* 2008; **10**(1): 15008–15015. DOI: 10.1088/1464-4258/10/01/015008

12. Green MA. *Third Generation Photovoltaics: Advanced Solar Energy Conversion*. Springer: Berlin, 2006; 4–5.

13. Würfel P. Solar energy conversion with hot electrons from impact ionisation. *Solar Energy Materials and Solar Cells* 1997; **46**(1): 43–52. DOI: 10.1016/S0927-0248(96)00092-X

14. Brown AS, Green MA. Detailed balance limit for the series constrained two terminal tandem solar cell. *Physica E: Low-dimensional Systems and Nanostructures* 2002; **14**(1–2): 96–100. DOI: 10.1016/S1386-9477(02)00364-8

15. Martí A, Araújo GL. Limiting efficiencies for photovoltaic energy conversion in multigap systems. *Solar Energy Materials and Solar Cells* 1996; **43**(2): 203–222. DOI: 10.1016/0927-0248(96)00015-3

16. Ries H. Complete and reversible absorption of radiation. *Applied physics. B, Lasers and optics* 1983; **32**(3): 153–156. DOI: 10.1007/BF00688821

17. Green MA. Third Generation Photovoltaics: Comparative Evaluation of Advanced Solar Conversion Options. *Proceedings of 29th IEEE Photovoltaic Specialists Conference*, New Orleans, 2002; 1330–1334.

18. Green MA. *Third Generation Photovoltaics: Advanced Solar Energy Conversion*. Springer: Berlin, 2006; 29–30.